Int. J. Electrochem. Sci., 13 **(2018)** 10088 – 10100, doi: 10.20964/2018.11.01

International Journal of ELECTROCHEMICAL SCIENCE
www.electrochemsci.org

The Predicted Dielectric Constant of an Amorphous PVDF Changing with Temperature by Molecular Dynamics Simulations

Taotao Hu[1,*], *Bingbing Hu*[2,*] *and Yabin Yan*[3,*]

[1] School of Highway, Chang'an University, Xi'an 710064, P. R. China.
[2] Faculty of Printing and Packing Engineering, Xi'an University of Technology, Xi'an 710048, P. R. China
[3] Institute of Systems Engineering, China Academy of Engineering Physics, Chengdu 621900, P. R. China
[*]E-mail: hutaotao@163.com, hubb416@xaut.edu.cn , yanyabin@gmail.com

Received: 2 July 2017 / *Accepted:* 14 August 2018 / *Published:* 1 October 2018

PVDF, a soft dielectric material, has attracted great attention in the research field of soft smart materials. However, some of the mechanisms for the dielectric and piezoelectric behaviors of PVDF are still not clear. In this work, the temperature dependent dielectric constant of the amorphous PVDF is predicted using molecular dynamics (MD) simulations. By inspecting the change of density with respect to temperature, the glass transition temperature (T_g) of the amorphous PVDF is successfully determined. To calculate the dielectric constant of PVDF, a constant electric field is applied to the simulation model at different temperatures. It is found that the applied electric field leads to the appearance of dipoles rotation. By increasing the strength of applied electric field, more dipoles rotate either along or against the direction of applied electric field. These dipoles rotation further results in the variation of polarization of PVDF. On the other hand, the dielectric constant is evaluated at different temperatures. The temperature is found to significantly affect the dielectric constant, and T_g plays a critical role as the critical temperature for material's dielectric constant. Moreover, the increment of the dielectric constant becomes much slower above T_g. This study explains the mechanism for the dielectric behavior of amorphous PVDF and provides a clue to the future study of other related properties of polymers, such as, piezoelectricity and flexoelectricity.

Keywords: PVDF; Polarization; Atomistic model; Dielectric constant

1. INTRODUCTION

Poly(vinylidene fluoride) (PVDF) mainly refers to the partial fluorine ethylene homopolymer or partial fluorine ethylene and other small amount of fluoride copolymer of vinyl monomer,

combining the characteristics of fluorine resin and general resin. PVDF has attracted great attention because of its piezoelectricity and electroactive properties,[1-3] and wide application in sensors, acoustic transducer, capacitor and random access memory.[4-7] In addition, the properties of amorphous PVDF are also of great interest, since PVDF often serves as the major component in a variety of amorphous fluoroelastomers such as Viton.[8, 9] At micron scale, the polar bonds play a primary role in the piezoelectricity and electroactive properties of PVDF. Actually, the chemical structure of polar PVDF molecules can be regarded as neutral alternating polyampholytes, which consists of alternating methylene and fluoro-methylene groups on the backbone, and carries net positive and net negative charges, respectively.[10, 11]

Up to now, extensive investigations have been conducted on the electrical properties of PVDF. In 1969, Kawai and Fukadalz found that the PVDF films, which was subjected to a uniaxial tension and a polarizing treatment through the high temperature and strong electric field, possessed the strongest piezoelectric effect among the synthesized polymer materials, and thus have a prominent industrial application.[1, 12] Bachmann investigated the variation of crystal phase of PVDF with the polarization of electric field. The transformation from the α to the β phase due to the polarization electric field was clarified through XRD analysis.[13] During polarization processing, the stronger the polarization electric field, the better the polarization effect. To improve the polarization effect, Ting used semiconductor ITO as the electrode material to achieve a higher polarized electric field that applied to PVDF film.[14] Rath and Levi added an appropriate amount of carbon nanotubes to PVDF, which apparently increased the proportion of β-phase and enhanced the piezoelectric constants.[15, 16] Moreover, by adding the barium carbonate to the PVDF matrix, Cherqaoui revealed the increment of both the dielectric constant and the dielectric loss of $BaTiO_3$/PVDF composites with the increase of $BaTiO_3$ volume proportion.[17]

Developing the novel materials with superior performance inevitably acquires a large amount of experiments with high cost and long time. Therefore, as an important supplement to experiments, computer simulations is a powerful tool to provide us with some crucial microstructural and kinetic information and a complete particle trajectory, which are difficult to be obtained experimentally. Thus, it is necessary to evaluate the variation characteristics of amorphous PVDF dielectric constant with temperature by using molecular dynamics (MD) simulations.

MD simulations have been widely adopted to investigate the electrical properties of PVDF. Ramos used a self-consistent quantum MD method to study the effects of electric field on both the α and β chains of PVDF, and the applied electric field mainly induces the chain reorientation, which means that the dipole moment with some smaller structural modifications is rearranged by the electric field.[18] Satyanarayana studied a PVDF phase change from α to β under stretching and polling using MD simulations, and the dipole orientation of the chain was found to be perpendicular to the direction of electric field.[19] Chen and Shew conducted Monte Carlo simulations to investigate two polar polymer models, i.e., the united atom model and the all-atom model, respectively. Because of different local chemical structures of these two models, different elongations of the main chain were found under the strong filed. The elongation of main chain of the all-atom model is relatively larger and the arrangement of the main chain molecules is more perpendicular to the electric field direction.[11] Therefore, the all-atom model provides a more accurate prediction to the rotation of methylene and

fluoro-methylene groups in the amorphous PVDF structure and the appearance of polarization under electric field. Bystrov investigated the molecular modeling and molecular dynamics of polarization switching for the ferroelectric films model of PVDF. Research results show that the rotation of chains at low external fields is not simultaneous (from one chain to another – similar as the kink propagation), the shift of electronic clouds is small and has little influence on the atomic nucleus. At high fields, the chains to rotate simultaneously, electron clouds have a large shift in a space relative to the atomic nucleus.[20] Chen studied the effect of electric field on the conformation of PVDF by MD. It was found that the H and F atoms of non-polarized PVDF chain distribute randomly, while for the polarized PVDF chain, most H and F atoms arrange along different sides of the backbone carbon atoms, which from local dipoles roughly along the direction of the applied electric field.[21] Paramonova calculated that the dielectric permittivity of the ultra-thin PVDF film is $\varepsilon = 2.4$using MD, while the dielectric permittivity of the bulk is $\varepsilon = 5\text{-}10$.[22] Maksimova and Maksimov also revealed that the impact of an external electric filed on the PVDF electrets results in the orientation of the crystallite polar axis along the field direction.[23] In addition, Young developed a computational method to calculate relaxation strength of an amorphous polymer solely according to its chemical structure. The dielectric relaxation strength model was established for polyimide, and the calculated dielectric relaxation strength was consistent with the experimental results. Additionally, it is clarified that both the pendant nitrile dipole and the backbone anhydride residue dipole make significant contributions to the polyimides' dielectric response.[24] Makowska-Janusik studied the electric field poling process of nonlinear optical chromophores embedded in an amorphous polymer matrix using MD simulations, and the electric field was found to greatly affect the local dynamics of PMMA segments and the flexibility of the torsional angle motion.[25]

The glass transition temperature (T_g) of polymer is the most important intrinsic property because it controls the range of temperatures for processing and application.[26] The glass transition temperature is the boundary between a glassy state and a high elastic state (rubber state). Below T_g, the polymer is in a glassy state. Both the motion of molecular chain and the segments are total constrained, and only the atoms (or groups) constituted molecules vibrate at their equilibrium position. At T_g, although the molecular chain is still unable to move, the chain segments becomes movable, resulting in the high elasticity of material. With rising temperature, the whole chain starts to move and leads to be the viscous flow properties.[27-29] It has been found that the temperature dependent properties of amorphous polymer, such as modulus, dielectric constant, enthalpy and specific heat change dramatically at T_g.[30, 31] Boucher investigated the polystyrene thin film by using dielectric spectroscopy (BDS), and found that the glass transition temperature was a linear cross-point temperature of fitting a straight line of the dielectric constant of the glassy state and the melting state.[32] This also means the mutation of dielectric constant of the amorphous polymer at T_g. However, to the author's knowledge, the effect of glass transition temperature on the dielectric constant of the amorphous PVDF has been rarely investigated by using MD simulations so far.

In this study, the variation of dielectric constant of amorphous PVDF with temperature is deeply investigated by MD simulations. The paper is organized as follows: In section 2, we describe the details of the model construction and simulation. In section 3, the results of MD simulations are discussed to analyze the variation of the polarization with the running time, temperature and electric

field strength in the presence of an applied electric field. Finally, the variation trend of dielectric constant of amorphous PVDF with temperature is summarized in section 4.

2. MODEL AND SIMULATION DETAILS

2.1 Force fields

Developing an accurate force field for molecular mechanics and molecular dynamics is critical important for the atomistic simulations. In this work, the energy expression is

$$U_{total} = U_{valence} + U_{nonbond}, \tag{1}$$

includes valence ($U_{valence}$) terms involving covalent bonds and long-range noncovalent interactions ($U_{nonbond}$). Here we take the covalent terms

$$U_{valence} = U_{bond}(l) + U_{angle}(\theta) + U_{torsion}(\phi), \tag{2}$$

to include bond stretch (U_{bond}), angle bend (U_{angle}), and dihedral angle torsion ($U_{torsion}$), where l, θ and ϕ represent the bond length, bond angle and dihedral angle, respectively.

Bond strength terms (U_{bond}) (Harmonic) in Eq. (2) can be expressed as

$$U_{bond}(l) = \frac{1}{2}k_l(l - l_0)^2, \tag{3}$$

Where l is the bond length, l_0 is the equilibrium bond length, and k_l is the force constant.

Angle bend terms (U_{angle}) (Harmonic) in Eq. (2) can be written as

$$U_{angle}(\theta) = \frac{1}{2}k_\theta(\theta - \theta_0)^2, \tag{4}$$

where θ is the angle between two bonds to a common atom, θ_0 is the equilibrium length, and k_θ is the force constant.

Torsion terms ($U_{torsion}$) (Harmonic) in Eq. (2) can be expressed as

$$U_{torsion}(\phi) = \frac{1}{2}V_{t,n}(1 + \cos(n\omega - \delta_n)), \tag{5}$$

where ϕ is the dihedral angle, $V_{t,n}$ is the height of the barrier for the torsion potential, δ_n is a phase factor, n is the rotation multiplicity associated with the rotational symmetry of the dihedral angle.

In Eq. (1), the nonbond terms is expressed as

$$U_{nonbond} = U_{vdW}(r_{ij}) + U_{Coulomb}(r_{ij}), \tag{6}$$

and consists of van der Waals ($U_{vdW}(r_{ij})$) and electrostatic ($U_{Coulomb}(r_{ij})$) terms, where r_{ij} is the distance between the i and j atoms.

Van der Waals term ($U_{vdW}(r_{ij})$) in Eq. (6) are modeled with the Lennard-Jones 12-6 potential, which can be written as

$$U_{vdW}(r_{ij}) = \frac{A_{ij}}{r_{ij}^{12}} - \frac{B_{ij}}{r_{ij}^{6}}, \tag{7}$$

where $A_{ij} = \sqrt{A_{ii}A_{jj}}$, $B_{ij} = \sqrt{B_{ii}B_{jj}}$.

Electrostatic term ($U_{Coulomb}\left(r_{ij}\right)$) can be expressed as

$$U_{Coulomb}\left(r_{ij}\right)=\frac{1}{4\pi\varepsilon_0}\frac{q_i q_j}{r_{ij}}+U_{extraneous\,term}\left(r_i\right), \quad (8)$$

where q_i is the charge on the i atomic center, ε_0 is the vacuum dielectric coefficient. Electrostatic interaction potential energy is a long-range force. In the presence of an external electric field, an addition term $U_{extraneous\,term}\left(r_i\right)$, which describes the interaction between the partial atomic charges and the applied electric field, is also involved in Eq. (8), the potential energy is calculated by the expression as

$$U_{extraneous\,term}\left(r_i\right)=\sum_i \vec{r}_i\cdot\vec{E}q_i, \quad (9)$$

where i is the atoms, q_i is the charge on atom i, $\vec{r}_i$ is the position vector of each group, and $\vec{E}$ is the applied electric field vector.

In this study, bond stretching, bond angle bending and dihedral angle torsion potential energy are represented by harmonic potentials. Parameter values are selected from the all-atom consistent valence force field (CVFF) in the Materials Studio software.[25, 33, 34] This force field has been used successfully to simulate a wide variety of chemical and biophysical systems, including different organic systems.[18, 35-37]

2.2 Simulation model

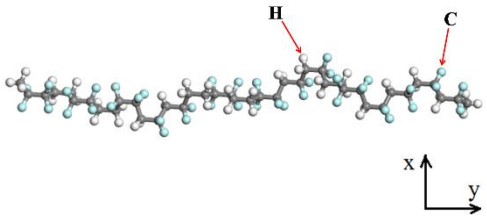

Figure 1. A chain of PVDF in configuration.

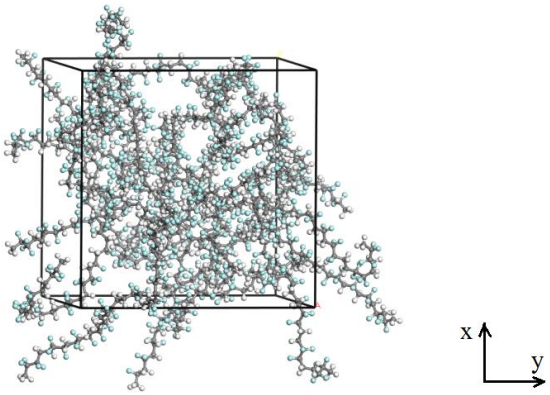

Figure 2. The configuration of an amorphous PVDF.

Since the polarizing process of amorphous PVDF closely involves the atom nature, it is essential to carry out study from both electronic and atomic aspects. In current work, the simulation model of amorphous PVDF is constructed by using the Materials Studio 7.0 software,[23] as shown in Figure 1 and 2. The model includes 20 randomly generated chains, and each chain consists of 20 CF_2-CF_2 monomer units. It has been found that when the chain length is greater than 17 monomer units, the dipole moment per monomer unit converges to a nearly constant value.[18] For the convenience of applying electric field and following simulations, a cube model with an edge length of 37.6175 Å is established, consisting of 2440 atoms. Initial polymer structure corresponding to a sample density of 0.8 g/cm^3 is generated. Simultaneous geometry optimization is adopted to optimize the structures, and the model is convert into data file which can be identified by LAMMPS software.[38] Finally, we apply the periodic boundary conditions and the electric fields to the model, and these systems are calculated in the LAMMPS software.

2.3 Glass transition temperature

After achieving an unpolarized equilibrium configuration by MD simulations, an external electric field is applied to the model, and the change of configuration in polarized state is carefully examined. The time step used in the simulation is approximately 1 fs. The Lennard-Jones and Coulomb interactions are calculated within the neighbor list with cutoff distance 0.95 nm. The long-range interactions are calculated in k-space as a particle-particle/particle-mesh solver (PPPM). The geometry-optimized structure is relaxed to obtain equilibrated structures by four steps. The first step is the relaxation for 1 ps under the condition of NVE. The second step is the relaxation for 20 ps under the condition of NVT. The third step is running for 250 ps at atmospheric pressure under NPT, and its temperature uniformly increases from 100 K to 400 K. The forth step is running for 250 ps at atmospheric pressure under NPT, and its temperature uniformly drop from 400 K to 100 K. After running a total of 521 ps, the total energy reaches an approximately constant value.

To determine a suitable temperature for the high-density-state simulation, the glass transition temperature (T_g) of the systems is estimated. The entire simulation process is in the NPT condition, where P=1, at different temperatures starting from 100 K up to 400 K in 50 K increments. The systems are firstly equilibrated for 100 ps at 100 K, and then for 20 ps at other temperatures. During entire calculation process, both densities and temperatures are recorded, and thus T_g is estimated from a density-temperature plot.

2.4 Applied electric fields

To comprehensively clarify the effect of temperature on the dielectric constant of amorphous PVDF, we apply the external electric fields with strengths of 0.025 V/Å to 0.15 V/Å along x direction, and the system runs for 3000 ps at different temperatures. The long durations of these simulations ensure that the model captures all of dipole reorientation and significant data for static analysis. The atomic charges and positions are used to calculate the total dipole moment of the simulation model at

every 100 steps, and the polarization is obtained by dividing the total dipole moment with the model volume.

The polarization expression is as follows

$$\vec{P} = \frac{\sum_i q_i \vec{r}_i}{V}, \tag{10}$$

where i labels the atoms, q_i and $\vec{r}_i$ are the charges and position vector, respectively.

The polarization emerges in dielectric and changes with external electric field. Polarization is the physical quantity that reflects this variation, representing the sum of the electric dipole moments in the unit volume with the unit of C/m^2. For the isotropic dielectric materials, the polarization $\vec{P}$ is proportional to the electric field strength $\vec{E}$, and the direction is the same,

$$\vec{P} = \chi \vec{E}, \tag{11}$$

where χ is the dielectric susceptibility.

Thus, the relative dielectric constant $\frac{\varepsilon}{\varepsilon_0}$ can be expressed as

$$\frac{\varepsilon}{\varepsilon_0} = 1 + \frac{\vec{P}}{\varepsilon_0 \vec{E}}, \tag{12}$$

where ε_0 is the vacuum dielectric coefficient, ε is the dielectric constant of material and usually depends on the material property and state parameters.[39]

3. RESULTS AND DISCUSSION

3.1 Glass transition temperature

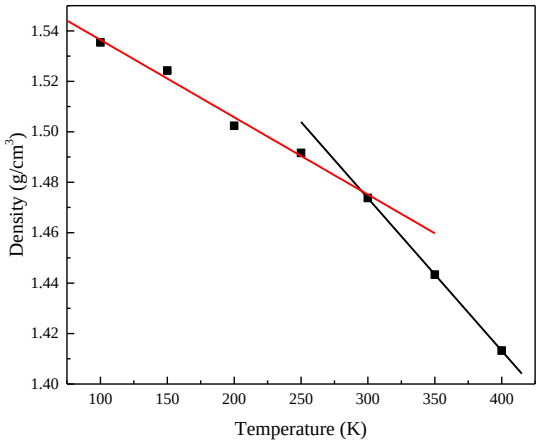

Figure 3. Density-temperature relationship for model.

The glass transition temperature (T_g) is determined from the density-temperature relationship. Figure 3 shows the variation of the density with different temperatures starting from 100 K up to 400 K in 50 K increments. There are two linear relations between the density and temperature,

corresponding to the temperature below and above T_g, respectively. The crossing point of two lines means the glass transition temperature. Therefore, the T_g of system is determined to be 295 K. Liu used a dynamic mechanical analysis (DMA) to measure the glass transition temperature of PVDF, which is 237 K.[40] Generally speaking, the T_g obtained by MD simulations are higher than those measured from experiments.[41] With comparison, the validity of current constructed model is approved. After determining the value of T_g, the variation of the dielectric constant at T_g is discussed in follows.

3.2 Dielectric properties

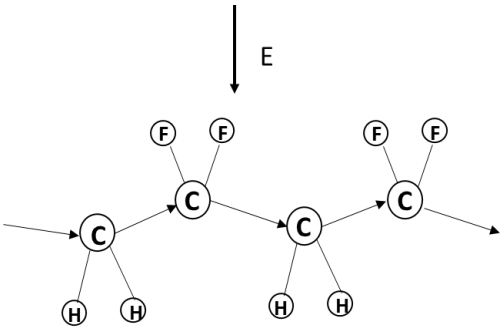

Figure 4. Changes in the molecular chain after applying an electric field.

A large number of studies have shown that the electric field has a significant polling effect, and causes the reorientation of dipolar moments,[18, 21, 23] as shown in Figure 4. Before applying electric field, the dipolar moments in the PVDF model randomly distribute in arbitrary direction (seen Figure 2), and thus no polarization exists. However, after applying electric fields, the dipolar moments show a preferential distribution along the direction of applied electric field. The CF_2 and CH_2 dipoles are coupled with the electric field, just as the dipoles rotate around the chain axis either along or against the direction of the applied electric field, and the main chains are accompanied with some minor structural modifications. Thus, the PVDF model has net dipole moments perpendicular to the polymer chain, pointing from the electronegative fluorine to the electropositive hydrogen. In other words, a rotation of CF_2 and CH_2 dipoles around the chain axis in opposite directions occurs with the applied electric fields, together with some minor structural modifications. Therefore, the polarization emerges in PVDF models.

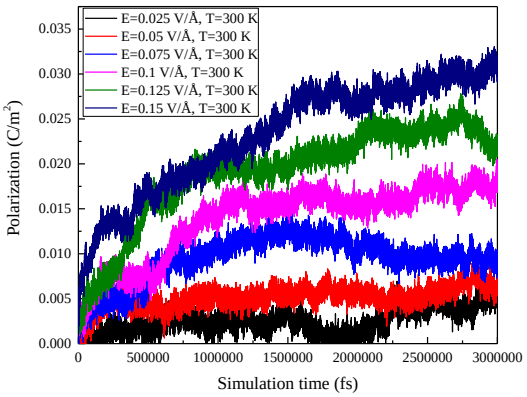

Figure 5. The variation of the polarization magnitude of the PVDF configuration with the running time under electric field with different strengths of 0.025 V/Å to 0.15 V/Å at 300 K.

Figure 5 depicts that the polarization magnitude of the PVDF configuration with the running time under electric field with different strengths of 0.025 V/Å to 0.15 V/Å along x axis direction at 300 K. As clearly shown in Figure 5, the variation trend of polarization is all most same, and the polarization enhances with the increment of electric field strength at 300 K. Furthermore, the magnitude of polarization increases with the running time and finally approaches to a constant value after 1500 ps. This phenomenon can be explained from subsequent aspects. After applying the electric field, a rotation of CF_2 and CH_2 around the chain axis in opposite directions occurs, which induces the appearance of dipole moments perpendicular to the polymer chain with the direction from the electronegative fluorine to the electropositive hydrogen. Thus, polarization emerges in the PVDF due to the effect of applied electric field. This is consistent with the previous theories and experimental studies on PVDF. In addition, a thermal motion in which atoms rotate randomly exists in amorphous PVDF. In contrast, after applying the electric field, the atom rotation aligns either along or against the direction of the applied electric field. By enhancing the applied electric field, the alignment of dipoles rotations along or against the applied electric field is strengthened. This dipole rotation further results in the change of system polarization.

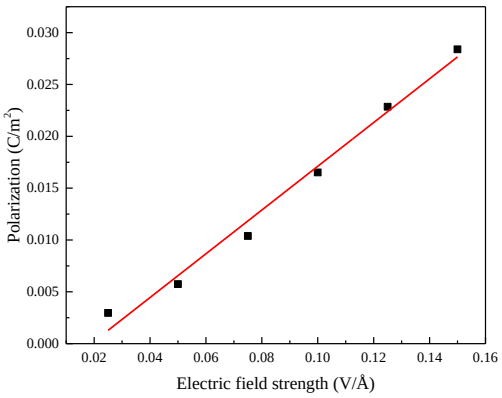

Figure 6. The averaged polarization of PVDF configuration after running 1500 ps under electric field with different strengths of 0.025 V/Å to 0.15 V/Å at 300 K.

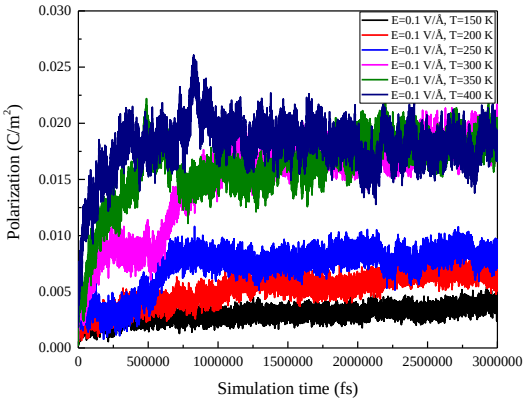

Figure 7. The variation of polarization magnitude of PVDF configuration with the running time at different temperatures of 150 K to 400 K under E=0.1 V/Å.

Figure 6 shows the averaged polarization of PVDF configuration after running 1500 ps under electric field with different strengths of 0.025 V/Å to 0.15 V/Å at 300 K. It can be found that the average of the polarization increases with the increment of electric field strength, and the magnitudes are basically proportional to each other.

Figure 7 presents the variation of polarization magnitude of PVDF configuration with the running time at different temperatures of 150 K to 400 K under E=0.1 V/Å. It is found that the polarization increases with rising temperature. Particularly, the apparent variation occurs near T_g. However, above T_g, the change of the polarization magnitude becomes smooth. This indicates that the glass transition temperature possesses a dominant influence on the polarization.

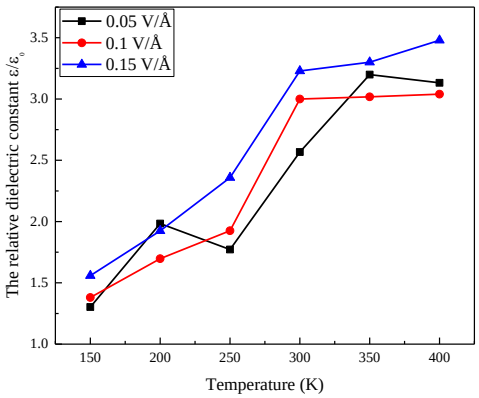

Figure 8. The variation of relative dielectric constant of PVDF with temperatures under different electric field strengths of 0.05 V/Å, 0.1 V/Å and 0.15 V/Å.

Figure 8 displays that the variation of relative dielectric constant of the PVDF with increasing the temperatures from 150 K to 400 K under different electric field strengths of 0.05 V/Å, 0.1 V/Å and 0.15 V/Å, respectively. The relative dielectric constant increases with the temperature rising from 150 K to 400 K. The magnitude changes dramatically near T_g, while the increase of dielectric constant becomes much slower above T_g. This conclusion well agrees with those of Bueche [30] and

Boucher.[32] There are several reasons to explain this phenomenon. The glass transition is a transition between a glassy state and a high elastic state (rubber state). From the viewpoint of molecular structure, the glass transition temperature is a slack phenomenon which is the amorphous part of the polymer from the frozen state to thawed state. Below T_g, the polymer is in the glass state, so that molecular chains and chain segments cannot move, and only the atoms (or groups) constituted molecules vibrate in the equilibrium position. However, due to the effect of applied electric field, only a small portion of the CF_2 and CH_2 dipoles on the main chain begins to rotate around the main chain along opposite direction. Thus, the PVDF produces electric polarization effect, but its value is small. When the temperature reaches T_g, although molecular chains are unable to move, chain segments becomes movable, leading to the high elasticity. By the applying the electric field, most of the CF_2 and CH_2 dipoles on the main chain rotate around the main chain in opposite direction. As temperatures rising further, the entire molecular chain begins to move, which shows the nature of viscous flow. Finally, almost all CF_2 and CH_2 dipoles rotate, and the relative dielectric constant calculated by polarization also tends to a stable value. Therefore, the relative dielectric constant changes dramatically near T_g, while the magnitude increment becomes much smaller above T_g. Meanwhile, it can be concluded that the strength of applied electric field has minor effect on the relative dielectric constant.

4. CONCLUSION

In this study, the amorphous PVDF changing with temperature is evaluated by molecular dynamics simulations. The glass transition temperature (T_g) of an amorphous PVDF is determined through the density-temperature relationship as 295 K, which is well consistent with previous experiments. To calculate the dielectric constant, a constant electric field is applied to the system at different temperatures. Due to the applied electric field, the CF_2 and CH_2 dipoles on the main chain rotate around the main chain along the opposite direction, and the amorphous PVDF is polarized. At 300 K, the variation trend of polarization value is basically same under different electric field strengths of 0.025 V/Å to 0.15 V/Å, and the polarization enhances with the increase of electric field strengths. All curves substantially become close to a constant value after running 1500 ps. It is also found that the averages of polarization increase with rising the strength of applied electric field after running 1500 ps, and they are basically proportional to each other. On the other hand, the dielectric constant of the amorphous PVDF is calculated at different temperatures from 150 K to 400 K. The temperature possesses a significant effect on the dielectric constant, where the dielectric constant increases as the temperature increasing. At higher temperatures, the barrier for the dipoles to rotate is lower, which allows more dipoles to rotate in response to the applied electric field. Thus, the dielectric constant calculated from the polarization is larger at higher temperature. In addition, T_g is found to be a critical point for material's dielectric constant. The relative dielectric constant changes dramatically near T_g, while the increase of the dielectric constant becomes much slower above T_g.

ACKNOWLEDGEMENTS

This work was supported by the National Natural Science Foundation of China (Grant No. 51705420).

References

1. H. Kawai, *J. Appl. Phys*., 8 (1969) 215.
2. P. Harnischfeger, B.J. Jungnickel, *J. Appl. Phys*., A50 (1990) 523.
3. T. Furukawa, *Phase Transit*., 18 (1989) 143.
4. K. Koga, H. Ohigashi, *J. Appl. Phys.,* 59 (1986) 2142.
5. B.T. Wang, R.L. Chen, *J. Intel. Mat. Syst. Str*., 11 (2000) 713.
6. G.M. Lloyd, Y. Zhang, P. Fabo, M.L. Wang, L. Wang, SPIE's 8th Annual International Symposium on Smart Structures and Materials, International Society for Optics and Photonics, 2001, p. 46.
7. D.Y. Kusuma, C.A. Nguyen, P.S. Lee, *J. Phys. Chem*., *B* 144 (2010) 13289.
8. S.B Lang, D.Q. Xiao, The Applications of Ferroelectric Polymers. IEEE xplore, 1988, P.251.
9. O.G. Byutner, G.D. Smith, *Macromolecules*, 32 (1999) 8376.
10. Y. Kantor, H. Li, M. Kardar, *Phys. Rev. Lett*., 69 (1992) 61.
11. Y. Chen, C.Y. Shew, *Chem. Phys. Lett*., 378 (2003) 142.
12. E. Fukada, S. Takashita, *Jap. J. Appl. Phys*., 8 (1969) 960.
13. M. Bachmann, W. Gordon, S. Weinhold, J. Lando, *J. Appl. Phys*., 51 (1980) 5095.
14. Y. Ting, H. Gunawan, A. Sugondo, C.W. hiu, *Ferroelectrics*, 446 (2013) 28.
15. N. Levi, R. Czerw, S. Xing, P. Iyer, D.L. Carroll, *Nano Lett*., 4 (2004) 1267.
16. S.K. Rath, S. Dubey, G.S. Kumar, S. Kumar, A.K. Patra, J. Bahadur, A.K. Singh, G. Harikrishnan, T.U. Patro. *J. mater. sci*., 49 (2014) 103.
17. B. Cherqaoui, J. Guillet, G. Seytre, *Rapid Comm*., 6 (1985).
18. M.M. Ramos, H.M. Correia, S. Lanceros-Mendez, *Comput. Mater. Sci*., 33 (2005) 230.
19. K.C. Satyanarayana, K .Bolton, *Polymer*, 53 (2012) 2927.
20. V.S. Bystrov. *Physica B,* 432 (2014) 21.
21. H.L. Chen, S.P. Ju, C.Y. Lin, C.T. Pan, *Comp. Mater. Sci*., 149 (2018) 217.
22. E.V. Paramonova, S.V. Filippov, V.E. Gevorkyan, L.A. Avakyan, X.J. Meng, B.B. Tian, *Ferroelectrics*, 509 (2017) 143.
23. O.G. Maksimova, A.V. Maksimov, *Ferroelectrics,* 501 (2016) 169.
24. J. Young, B. Farmer, J. Hinkley, *Polymer*, 40 (1999) 2787.
25. M. Makowska-Janusik, H. Reis, M.G. Papadopoulos, I. Economou, N. Zacharopoulos, *J. Phys Chem. B*, 108 (2004) 588.
26. P. Meares, Polymers: structure and bulk properties, Van Nostrand Reinhold, USA, 1965.
27. N. McGrum, B. Read, G. Williams, Anelastic and dielectric effects in polymeric solids, Wiley, USA, 1967.
28. K.J. Zeleznak, R.C. Hoseney, Cereal. Chem., 64 (1987) 121.
29. L.H. Sperling, Introduction to Physical Polymer Science, John Wiley & Sons, USA, 2005.
30. F. Bueche, Physical properties of polymers, Interscience Publishers, 1962.
31. R.A. Gerasimov, V.I. Egorov, O.G. Maksimova, T.O. Petrova, A.V. Maksimov, *Ferroelectrics*, 525 (2018) 93.
32. V.M. Boucher, D. Cangialosi, H. Yin, A. Schönhals, A. Alegría, J. Colmenero, *Soft Matter*., 8 (2012) 5119.
33. A. Hagler, S. Lifson, *J. Am. Chem. Soc*., 96 (1974) 5327.
34. D.H. Kitson, A.T. Hagler, *Biochem.*, 27 (1988) 5246.
35. P. Dauber-Osguthorpe, V.A. Roberts, D. J. Osguthorpe, J. Wolff, M. Genest, *Proteins*, 4 (1988) 31.
36. K.F. Lau, H.E. Alper, T.S, Thacher, T.R. Stouch, *J. Phys. Chem.*, 98 (1994) 8785.
37. H. David. A.T. Kitson, *Biochem.*, 27 (1988) 5246.
38. S. Plimpton, *J. Comp. Phys*., 117 (1995) 1.
39. C. Wang, J. Li, M. Zhao, Piezoelectric ferroelectric physics, Science Press, China, 2009.

40. T.Y. Liu, W.C. Lin, L.Y. Huang, S.Y. Chen, M.C. Yang, *Polym. Advan. Technol.*, 16 (2005) 413.
41. Y. Tu, Q. Zhang, H. Ågren, *J. Phys. Chem. B*, 111 (2007) 3591.